

Experimental studies of Bose-Einstein condensation

Dallin S. Durfee and Wolfgang Ketterle

Department of Physics and Research Laboratory of Electronics, Massachusetts Institute of Technology, Cambridge, MA 02139

dallin@amo.mit.edu

Abstract: We describe several experimental studies of Bose-Einstein condensation in a dilute gas of sodium atoms. These include studies of static and dynamic behavior of the condensate, and of its coherence properties.

©1998 Optical Society of America

OCIS codes: (020.0020) Atomic and molecular physics; (020.7010) Trapping; (999.9999) Bose-Einstein condensation

References and links

1. M.H. Anderson, J.R. Ensher, M.R. Matthews, C.E. Wieman, and E.A. Cornell, "Observation of Bose-Einstein Condensation in a Dilute Atomic Vapor", *Science* **269**, 198 (1995).
2. K.B. Davis, M.-O. Mewes, M.R. Andrews, N.J. van Druten, D.S. Durfee, D.M. Kurn, and W. Ketterle, "Bose-Einstein condensation in a gas of sodium atoms", *Phys. Rev. Lett.* **75**, 3969 (1995).
3. C.C. Bradley, C.A. Sackett, and R.G. Hulet, "Bose-Einstein Condensation of Lithium: Observation of Limited Condensate Number", *Phys. Rev. Lett.* **78**, 985 (1997).
4. K. Huang, "Imperfect Bose Gas", in *Studies in Statistical Mechanics*, vol. II, edited by J. de Boer and G.E. Uhlenbeck (North-Holland, Amsterdam, 1964) p. 3.
5. A. Griffin, D.W. Snoke, and S. Stringari (editors), *Bose-Einstein Condensation* (Cambridge University Press, Cambridge, 1995).
6. K. Huang, *Statistical Mechanics*, second edition (Wiley, New York, 1987).
7. M.-O. Mewes, M.R. Andrews, N.J. van Druten, D.M. Kurn, D.S. Durfee, and W. Ketterle, "Bose-Einstein condensation in a tightly confining dc magnetic trap", *Phys. Rev. Lett.* **77**, 416 (1996).
8. Background information for the 1997 Nobel prize in physics for laser cooling, <http://www.nobel.se/announcement-97/phyback97.html>
9. Links to research groups with atom traps, <http://www-atoms.physics.wisc.edu/OtherSites.html>
10. C.G. Townsend, N.J. van Druten, M.R. Andrews, D.S. Durfee, D.M. Kurn, M.-O. Mewes, and W. Ketterle, "Bose-Einstein condensation of a weakly-interacting gas", in *Ultracold Atoms and Bose-Einstein-Condensation, 1996*, K. Burnett, ed., OSA Trends in Optics and Photonics Series, Vol. 7 (Optical Society of America, Washington D.C., 1996) p. 2.
11. Indirect evidence was reported in: C.C. Bradley, C.A. Sackett, J.J. Tollet, and R.G. Hulet, "Evidence of Bose-Einstein Condensation in an Atomic Gas with Attractive Interactions", *Phys. Rev. Lett.* **75**, 1687 (1995).
12. W. Ketterle, M.R. Andrews, K.B. Davis, D.S. Durfee, D.M. Kurn, M.-O. Mewes, and N.J. van Druten, "Bose-Einstein condensation of ultracold atomic gases", *Phys. Scr.* **T66**, 31 (1996).
13. BEC home page of the Georgia Southern University, <http://amo.phy.gasou.edu/bec.html>
14. Home page of our group, <http://amo.mit.edu/~bec>
15. N.J. van Druten, C.G. Townsend, M.R. Andrews, D.S. Durfee, D.M. Kurn, M.-O. Mewes, and W. Ketterle, "Bose-Einstein condensates - a new form of quantum matter", *Czech. J. Phys.* **46 (S6)**, 3077 (1996).
16. D.S. Jin, J.R. Ensher, M.R. Matthews, C.E. Wieman, and E.A. Cornell, "Quantitative Studies of Bose-Einstein Condensation in a Dilute Atomic Vapor", *Czech. J. Phys.* **46 (S6)**, 3070 (1996).
17. C.A. Sackett, C.C. Bradley, M. Welling, and R.G. Hulet, "Bose-Einstein Condensation of Lithium", *Braz. J. Phys.* **27**, 154 (1997).
18. N.P. Proukakis, K. Burnett, M. Edwards, R.J. Dodd, and C.W. Clark, "Theory of Bose-Einstein condensed trapped atoms", in *Ultracold Atoms and Bose-Einstein-Condensation, 1996*, K. Burnett, ed., OSA Trends in Optics and Photonics Series, Vol. 7 (Optical Society of America, Washington D.C., 1996) p. 14.
19. A. Einstein, "Quantentheorie des einatomigen idealen Gases. II", *Sitzungsber. K. Preuss. Akad. Wiss. Phys. Math. Kl.*, 3 (1925).

20. M.R. Andrews, M.-O. Mewes, N.J. van Druten, D.S. Durfee, D.M. Kurn, and W. Ketterle, "Direct, Non-Destructive Observation of a Bose Condensate", *Science* **273**, 84 (1996).
21. M.R. Andrews, D.M. Kurn, H.-J. Miesner, D.S. Durfee, C.G. Townsend, S. Inouye, and W. Ketterle, "Propagation of sound in a Bose-Einstein condensate", *Phys. Rev. Lett.* **79**, 553 (1997).
22. E. Hecht, *Optics*, 2nd edition (Addison-Wesley, Reading, 1989).
23. Y. Castin and R. Dum, "Bose-Einstein condensation in time dependent traps", *Phys. Rev. Lett.* **77**, 5315 (1996).
24. A. Griffin, *Excitations in a Bose-condensed liquid* (Cambridge University Press, Cambridge, 1993).
25. D.S. Jin, J.R. Ensher, M.R. Matthews, C.E. Wieman, and E.A. Cornell, "Collective Excitations of a Bose-Einstein Condensate in a Dilute Gas", *Phys. Rev. Lett.* **77**, 420 (1996).
26. M.-O. Mewes, M.R. Andrews, N.J. van Druten, D.M. Kurn, D.S. Durfee, C.G. Townsend, and W. Ketterle, "Collective Excitations of a Bose-Einstein condensate in a Magnetic Trap", *Phys. Rev. Lett.* **77**, 988 (1996).
27. S. Stringari, "Collective excitations of a trapped Bose-condensed gas", *Phys. Rev. Lett.* **77**, 2360 (1996).
28. D. Stamper-Kurn, H.-J. Miesner, S. Inouye, M.R. Andrews, and W. Ketterle, "Excitations of a Bose-Einstein Condensate at Non-Zero Temperature: A Study of Zeroth, First, and Second Sound", *Phys. Rev. Lett.* (1998), submitted.
29. D.S. Jin, M.R. Matthews, J.R. Ensher, C.E. Wieman, and E.A. Cornell, "Temperature-Dependent Damping and Frequency Shifts in Collective Excitations of a Dilute Bose-Einstein Condensate", *Phys. Rev. Lett.* **78**, 764 (1997).
30. H.M. Wiseman, "Defining the (atom) laser", *Phys. Rev. A* **56**, 2068 (1997).
31. D. Kleppner, *Phys. Today*, Aug. 1997, p. 11; Jan. 1998, p. 90.
32. M.-O. Mewes, M.R. Andrews, D.M. Kurn, D.S. Durfee, C.G. Townsend, and W. Ketterle, "Output coupler for Bose-Einstein condensed atoms", *Phys. Rev. Lett.* **78**, 582 (1997).
33. P.W. Anderson, "Measurement in Quantum Theory and the Problem of Complex Systems", in *The Lesson of Quantum Theory*, J.d. Boer, E. Dal, and O. Ulfbeck, ed. (Elsevier, Amsterdam, 1986) p. 23.
34. J. Javanainen and S.M. Yoo, "Quantum Phase of a Bose-Einstein Condensate with an Arbitrary Number of Atoms", *Phys. Rev. Lett.* **76**, 161 (1996).
35. M.R. Andrews, C.G. Townsend, H.-J. Miesner, D.S. Durfee, D.M. Kurn, and W. Ketterle, "Observation of interference between two Bose condensates", *Science* **275**, 637 (1997).
36. W. Ketterle and H.-J. Miesner, "Coherence properties of Bose-Einstein condensates and atom lasers", *Phys. Rev. A* **56**, 3291 (1997).
37. E.A. Burt, R.W. Ghrist, C.J. Myatt, M.J. Holland, E.A. Cornell, and C.E. Wieman, "Coherence, Correlations, and Collisions: What One Learns About Bose-Einstein Condensates from Their Decay", *Phys. Rev. Lett.* **79**, 337 (1997).
38. P. Navez, D. Bitouk, M. Gajda, Z. Idziaszek, and K. Rzazewski, "Fourth Statistical Ensemble for the Bose-Einstein Condensate", *Phys. Rev. Lett.* **79**, 1789 (1997).
39. P.A. Ruprecht, M.J. Holland, K. Burnett, and M. Edwards, "Time-dependent solution of the nonlinear Schrödinger equation for Bose-condensed trapped neutral atoms", *Phys. Rev. A* **51**, 4704 (1995).
40. Y. Kagan, G.V. Shlyapnikov, and J.T.M. Walraven, "Bose-Einstein condensation in trapped atomic gases", *Phys. Rev. Lett.* **76**, 2670 (1996).

1. Introduction

The recent observation of Bose-Einstein condensation (BEC) in alkali vapors [1-3] was the realization of many long-standing goals: (1) To cool neutral atoms into the ground state of the system, thus exerting ultimate control over the motion and position of atoms limited only by Heisenberg's uncertainty relation. (2) To generate a coherent sample of atoms all occupying the same quantum state (this was used to realize a rudimentary atom laser, a device which generates coherent matter waves). (3) To produce degenerate quantum gases with properties quite different from the quantum liquids He-3 and He-4. This provides a testing ground for many-body theories of the dilute Bose gas which were developed many decades ago but never tested experimentally[4]. BEC of dilute atomic gases or of excitons is a macroscopic quantum phenomena with similarities to superfluidity, superconductivity and the laser phenomenon[5].

Bose-Einstein condensation is based on the wave nature of particles, which is at the heart of quantum mechanics. In a simplified picture, atoms in a gas may be regarded as quantum-mechanical wavepackets which have an extent on the order of a thermal de Broglie wavelength (the position uncertainty associated with the thermal momentum distribution). The lower the temperature, the longer is the de Broglie wavelength. When atoms are cooled to the point where the thermal de Broglie wavelength is comparable to the interatomic separation, then the atomic wavepackets "overlap" and the indistinguishability of particles

becomes important (Fig. 1). Bosons undergo a phase transition and form a Bose-Einstein condensate, a dense and coherent cloud of atoms all occupying the same quantum mechanical state[6]. The relation between the transition temperature and the peak atomic density n can be simply expressed as $n\lambda_{dB}^3 = 2.612$, where the thermal de Broglie wavelength is defined as $\lambda_{dB} = (2\pi\hbar^2/mk_B T)^{1/2}$ and m is the mass of the atom.

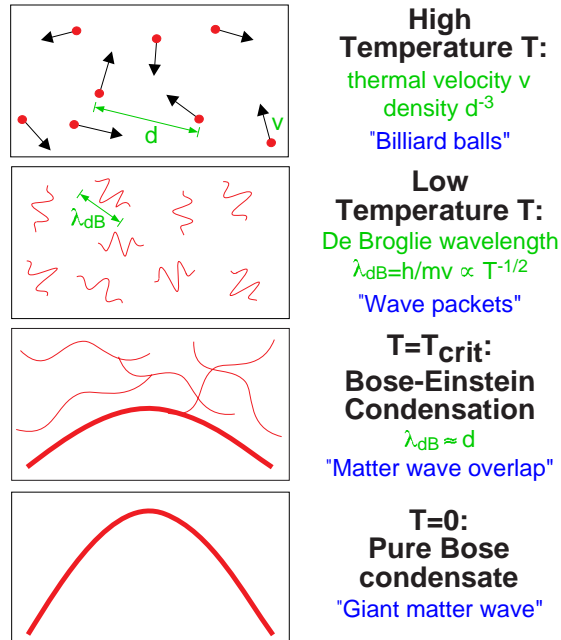


Fig. 1. Criterion for Bose-Einstein condensation. At high temperatures, a weakly interacting gas can be treated as a system of “billiard balls”. In a simplified quantum description, the atoms can be regarded as wavepackets with an extension Δx , approximately given by Heisenberg’s uncertainty relation $\Delta x = \hbar/\Delta p$, where Δp denotes the width of the thermal momentum distribution. Δx is approximately equal to the thermal de Broglie wavelength λ_{dB} , the matter wavelength for an atom moving with the thermal velocity. When the gas is cooled down the de Broglie wavelength increases. At the BEC transition temperature, λ_{dB} becomes comparable to the distance between atoms, and the Bose condensate forms which is characterized by a macroscopic population of the ground state of the system. As the temperature approaches absolute zero, the thermal cloud disappears leaving a pure Bose condensate.

The realization of Bose-Einstein condensation requires techniques to cool gases to sub-microkelvin temperatures and atom traps to confine them at high density and keep them away from the hot walls of the vacuum chamber. Over the last 15 years, such techniques have been developed in the atomic physics and low-temperature communities[5]. The MIT experiment uses a multistage process to cool hot sodium vapor down to temperatures where the atoms form a condensate[2,7]. A beam of sodium atoms is emitted from an atomic beam oven at a density of about 10^{14} atoms per cm^3 , similar to the eventual density of the condensate. The gas is cooled by nine orders of magnitude from 600K to $1\mu\text{K}$ by first slowing the atomic beam, then by optical trapping and laser cooling the atoms[8,9], and finally by magnetic trapping and evaporative cooling[10].

The first experimental demonstrations of BEC [1-3, 11] were followed by several experimental studies and numerous theoretical papers (See Refs. [10, 12-18] for reviews). We refer to our previous review[10] for the historical context, for an account of the developments which led to BEC, and for an overview of the techniques used to realize BEC. In this paper, we summarize some experimental studies of Bose-Einstein condensation and illustrate them with animations of experimental results. These illustrations display another important aspect

of Bose-Einstein condensation. Since a Bose condensate is characterized by a macroscopic population of a single quantum state, the imaging of condensates and their dynamical behavior constitutes a dramatic visualization of quantum-mechanical wavefunctions and give wavefunctions a new level of reality. The animations and many figures in this paper have not been published before, whereas all experimental results have been previously reported in more technical papers.

2. Identifying the Bose-Einstein condensate

Bose-Einstein condensation was achieved by evaporatively cooling a gas of magnetically trapped atoms to the transition temperature. In the first observations[1,2], four features were used to identify the formation of a Bose-Einstein condensate :

- (1) The sudden increase in the density of the cloud.
- (2) The sudden appearance of a bimodal cloud consisting of a diffuse normal component and a dense core (the condensate).
- (3) The velocity distribution of the condensate was anisotropic in contrast to the isotropic expansion of the normal (non-condensed) component.
- (4) The good agreement between the predicted and measured transition temperatures.

The first three points are illustrated in Fig. 2. It shows time-of-flight pictures of expanding clouds released from the magnetic trap by suddenly switching off the trap. These images, taken during our second data run which produced Bose-Einstein condensation, were recorded by illuminating the cloud with resonant laser light and imaging the shadow of the cloud onto a CCD camera[2].

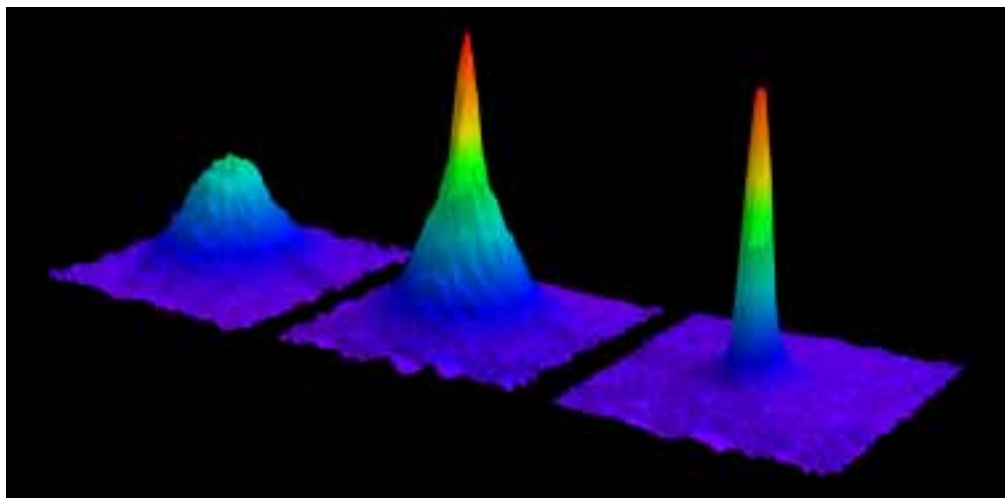


Fig. 2. Observation of Bose-Einstein condensation by absorption imaging. Shown is absorption vs. two spatial dimensions. The Bose-Einstein condensate is characterized by its slow expansion observed after 6 msec time of flight. The left picture shows an expanding cloud cooled to just above the transition point; middle: just after the condensate appeared; right: after further evaporative cooling has left an almost pure condensate. The width of the images is 1.0 mm. The total number of atoms at the phase transition is about 7×10^5 , the temperature at the transition point is 2 μ K.

The animation in Fig. 3 shows the suddenness of the formation of the condensate. Each frame required a new loading and cooling cycle. Frames were taken for various final frequencies of the rf sweep which controlled the evaporative cooling process. To a very good approximation, the temperature of the cloud is linearly related to the final rf frequency. Discrete frames were interpolated in such a way that the rf frequency decreases at a constant rate during the length of the animation. Since close to the phase transition the radiofrequency

was swept linearly in time, Fig. 3 represents the temporal dynamics of the cooling process during the last fraction of a second (the whole evaporation process took only seven seconds).

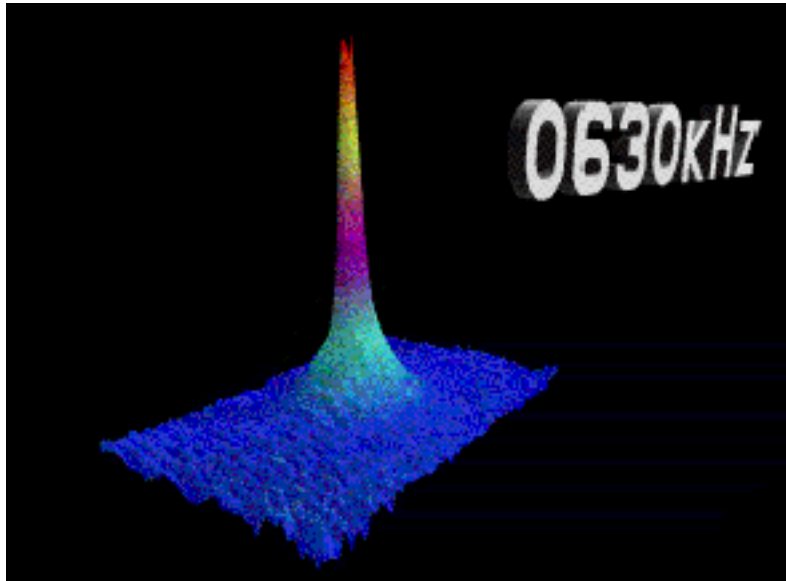


Fig. 3. Formation of a Bose-Einstein condensate. Two-dimensional probe absorption images, after 6 msec time of flight, show the sharpness of the phase transition. This sequence includes the three images of Fig. 2. The evaporative cooling was induced by an externally applied rf field. As the final rf frequency (labeled on the plots) was lowered, lower temperatures and higher phase space densities were reached. The cloud at the start of the animation had a temperature of about 5 μ K. Above the phase transition (frequency >700 kHz) the clouds expanded spherically, as expected for a normal thermal distribution. As the frequency was reduced, the spherical cloud shrank in size, due to the lower temperatures reached. Below the transition point (frequency <700 kHz, 2 μ K) an elliptical core appeared, which is the signature of the condensate. As the frequency was lowered the spherical part became invisible, corresponding to a pure condensate. Finally, when the threshold for evaporation reached the bottom of the trap (around 300 kHz), the condensate itself was lost by evaporation. Note that the color scale here has been chosen to represent optical density (OD) instead of absorption (A), as used in the other images. The two are related by $OD = -\ln(1-A)$. The rf frequency displayed in the animation changes when a new original frame is displayed and stays constant when interpolated frames are shown. The size of the frame is 1.1 by 1.6 mm.

Fig. 4 shows the formation of the condensate observed by directly imaging the trapped condensate. One can regard Figures 2 and 3 as showing condensation in energy (or momentum space), whereas Fig. 4 demonstrates that condensation also takes place in configuration space. BEC is always a condensation phenomenon into the lowest energy state. In a homogeneous gas, however, the ground state has the same spatial extension as the excited state - therefore BEC is only a condensation in momentum space. In contrast, in a harmonic oscillator potential the ground state has the smallest extension, and one can observe BEC in configuration space. In his second paper on quantum statistics, Einstein used the notion of the saturated ideal gas to describe the condensation phenomenon[19]. Fig. 4 shows directly the “droplet” formation when the atomic vapor reaches “quantum saturation.”

Spatial images like the one in Fig. 4 are not taken by absorption imaging, but by dispersive imaging[20, 21]. The reason for this is that the trapped condensates are very dense. If the image were to be taken on resonance, the probe light would be fully absorbed, and close to resonance, it would be strongly refracted due to the index of refraction of the trapped cloud. A solution is to go far off resonance (in our case about 350 half linewidths) where absorption is negligible and dispersion is small, and use imaging techniques which

image the spatial distribution of the index of refraction. Techniques such as dark-ground imaging and phase-contrast imaging are well known in microscopy[22] and can be applied to the imaging of atoms. A major advantage of dispersive over absorptive imaging is that one can obtain much higher signal levels for the same amount of heating. In dispersive imaging, one collects the photons which have been elastically scattered into the forward direction. The momentum transfer due to this scattering is negligible. Instead, the major heating mechanism in dispersive imaging is due to large angle Rayleigh scattering. The ratio of the rates for elastic scattering and Rayleigh scattering are proportional to the (resonant) optical density, which is about 200 in our case. Therefore, one can image about two orders of magnitude more dispersively scattered photons than absorbed photons for the same amount of heating. Since dispersive imaging is almost non-destructive, it can be used to record “real-time movies” of the dynamics of a condensate by using multiple probe laser pulses in combination with a fast CCD camera.

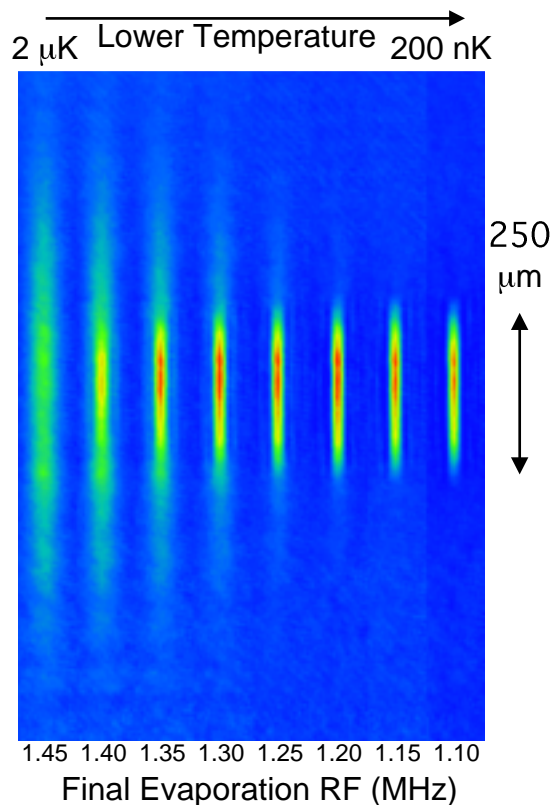


Fig. 4. Direct observation of the formation of a Bose-Einstein condensate using dispersive light scattering (phase contrast images). The intensity of the scattered light is a measure of the density of atoms (integrated along the line-of-sight). The left picture shows the cloud slightly above the BEC transition temperature. When the temperature was lowered, a dense core formed in the center of the trap - the Bose condensate. Further cooling increased the condensate fraction to close to 100% (right).

Fig. 5 shows the expansion of a mixed cloud, demonstrating the different properties of a condensate and the normal component. The frames were recorded by varying the time-of-flight in successive cooling cycles. They show atoms released from the cloverleaf magnetic trap[7]. At early times the cloud is optically dense and absorbs almost all of the incident light (red color). Between 10 and 25 msec one can clearly see the isotropic expansion of the thermal cloud. This reflects the fact that the velocity distribution of a gas is isotropic irrespective of the shape of the container. In contrast, the condensate shows a strong

anisotropy in the expansion related to the anisotropy of the magnetic confinement. A condensate of an ideal non-interacting gas occupies the ground state of the system. The width of the velocity distribution of the expanding cloud is given by Heisenberg's uncertainty relation and is inversely proportional to the spatial extension of the ground state wavefunction. As a result, the aspect ratio of an expanding condensate approaches the inverse aspect ratio of the trapped condensate. For a weakly interacting condensate, the situation is different because the repulsion between the atoms weakens the trapping potential and leads to a larger size of the condensate. After the trap is switched off, the internal energy (mean-field energy) is converted into kinetic energy in an anisotropic way: the accelerating force due to the internal mean field energy is proportional to the gradient of the mean field energy and therefore proportional to the density gradient. This means that for an initially cigar shaped cloud, the radial acceleration is much larger than the axial one, and the aspect ratio of a freely expanding condensate inverts. For very long expansion times, the aspect ratio was predicted to be $(\pi/2)$ times the inverse of the aspect ratio of the trapped cloud[23].

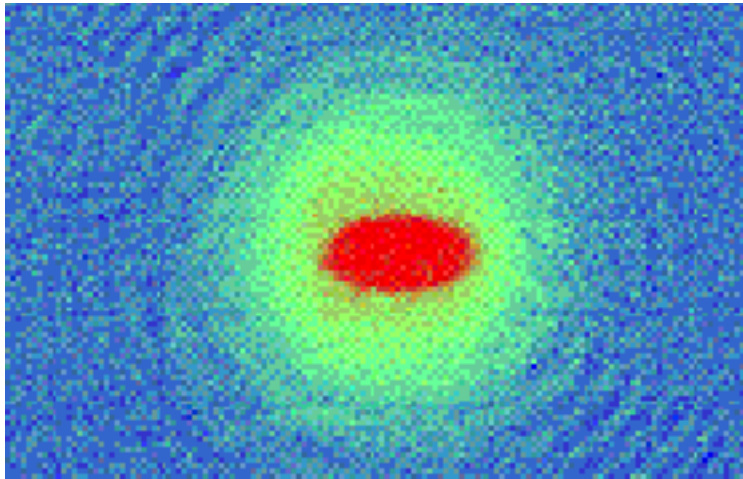


Fig. 5. Time-of-flight expansion of a Bose condensate. The first observations of BEC were made by suddenly turning off the trapping fields and allowing the atoms to expand ballistically. Absorption images were taken after a variable delay time. The earliest images show the pencil-like shape of the initial cloud. In the early phase of the expansion, the clouds appeared larger than their true sizes due to complete absorption of the probe laser light. Between 10 and 25 msec, the isotropic expansion of the normal component was observed. After 15 msec, the slower strongly anisotropic expansion of the Bose condensate became visible. At 60 msec, the signal was lost because the clouds had fallen almost 2 cm due to gravity. They were no longer illuminated by an optical pumping beam, which transferred the atoms from the lower to the upper hyperfine state, where they are detected by absorption imaging. When the cloud has expanded to many times its original size, such time-of-flight images represent the velocity distribution of the released cloud (in this figure, this applies only to the radial expansion). The width of the field of view is 1.8 mm.

3. Collective excitations of a Bose condensate

Collective excitations of liquid helium played a key role in determining its superfluid properties[24]. It is now well understood that the phonon-nature of the low-lying excitations imply superfluidity up to a critical velocity which is given by the speed of sound. The low-lying excitations of a trapped Bose condensate show discrete modes due to the small finite size of the trapped sample. They correspond to standing sound waves. The few lowest-lying excitations were studied in Boulder[25] and at MIT [26].

Fig. 6 shows our first observation of collective excitations. The cloud is contracting along the axial direction while expanding radially and vice versa and therefore corresponds to

a quadrupole mode of a spherical cloud. The oscillations were excited with a time-dependent modulation of the trapping potential. A variable time delay was introduced between the excitation and the release of the cloud. In this way, the free time evolution of the system after the excitation was probed. The cloud was observed by absorption imaging after a sudden switch-off of the magnetic trap and 40 msec of ballistic expansion. The measured frequency of oscillation were in excellent agreement with predictions based on the non-linear Schroedinger equation[27, 28].

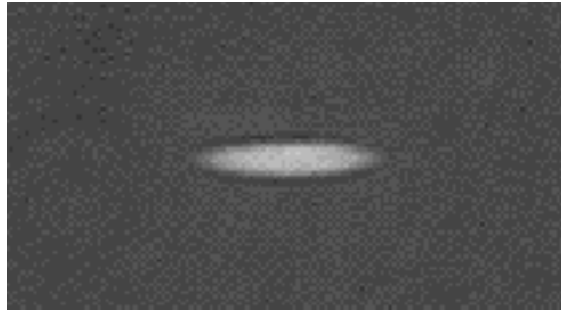


Fig. 6. Observation of collective excitations. The first studies of collective excitations in a dilute Bose condensate were done using time-of-flight imaging. In this example, the condensate was driven by modulating the strength of the magnetic trap. Then, after the condensate oscillated freely for a variable amount of time, the trap was turned off allowing the condensate to ballistically expand. By stringing together many time-of-flight pictures, a movie was created which shows the free oscillation of the trapped condensate. For very long time-of-flight and an ideal gas, the observed shape oscillations reflect oscillations of the velocity distribution of the trapped condensate. In the case shown here, they depend on both the initial spatial and velocity distributions. From such data the frequency and damping rate of the excitation was determined. The width of the field of view is 3.3 mm.

In order to understand the observed damping time of 250 msec, studies have recently been extended to finite temperatures[28, 29]. Our studies were done using direct observation of the spatial oscillation by dispersive imaging. Since this method is much less destructive than absorption imaging, “real-time movies” with up to 30 pictures of the same oscillating condensate could be taken. Fig. 7 shows the observation of the axial dipole motion (center of mass motion) which was excited by periodically moving the center of the magnetic trap. The dipole motion is undamped in a harmonic trapping potential. Although the dipole mode by itself doesn’t reveal anything about the nature of the Bose condensate, an accurate measurement of its frequency is important since it is needed to normalize the other collective excitation frequencies in order to compare them with theory. Images like those in Fig. 7 allow a single-shot determination of trapping frequencies with 0.2 % precision.

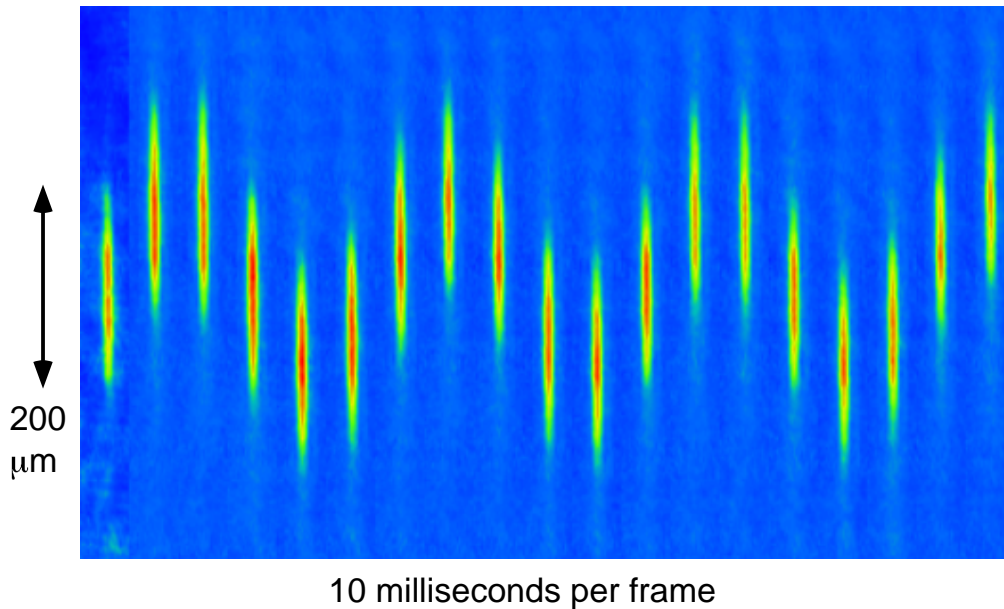


Fig. 7. Phase contrast images of the dipole oscillation. Using non-destructive techniques, the dipole oscillation was observed directly for a single trapped condensate. This oscillation is a collective “sloshing” of the entire cloud back and forth in the trap. The frames were taken with a separation of 10 msec between frames. The length of the condensate was 200 μm . From these images, the frequency of the dipole motion was determined to be 19 Hz.

When the cloud was excited by modulating the axial confinement, the quadrupole-type oscillation could be observed in the spatial domain (Fig. 8). In Fig. 9, thirteen pictures like Fig. 8 but with various delays were combined into an animation. It shows the dynamics of the condensate over a period of one second. One can clearly see the damping of the oscillations of the shape of the condensate, whereas the center-of-mass motion is undamped. Several theoretical schemes have recently been developed to describe the damping of collective excitations as a function of temperature (see references in [28]).

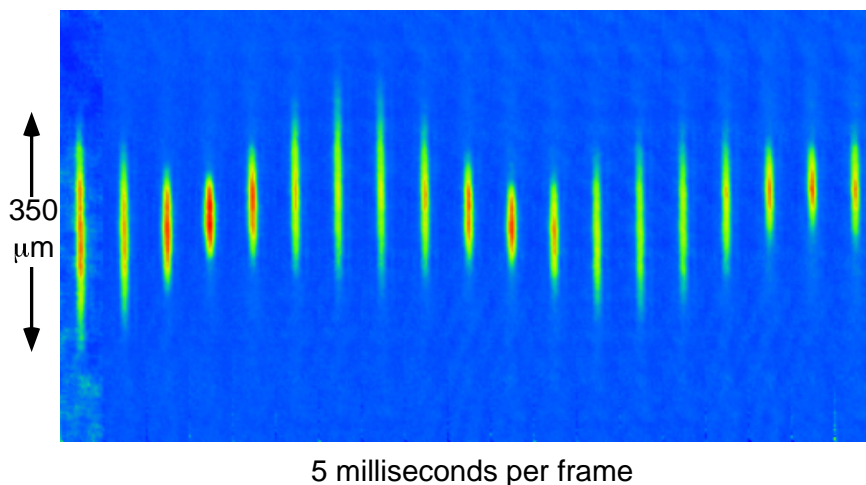


Fig. 8. Phase contrast images of the quadrupole-type shape oscillation. In this mode, the radial width and the axial length of the condensate oscillate out of phase. The images were taken of a single condensate at a rate of 200 frames per second. From this data, the frequency of the shape oscillation was determined to be 30 Hz.

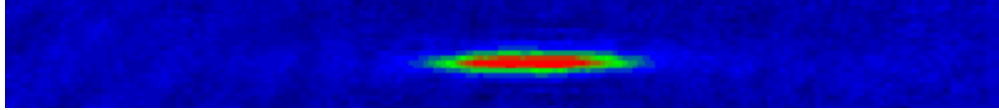


Fig. 9. "Real time" movie of the oscillations of a Bose-Einstein condensate. Frames in the movie were taken at a rate of 200 per second, and played back at 10 frames per second. Beginning in the first frame, the condensate was excited by a 3 cycle 30 Hz modulation of the trapping potential. Both the quadrupole-type "shape" oscillation (Fig. 8) and the dipole "sloshing" oscillation (Fig. 7) were excited. Near the end of the movie, the shape oscillation had damped away, but the undamped dipole oscillation continued. The damping time of the quadrupole-type mode has been determined to be about 250 msec.

4. Realization of an atom laser

An atom laser is a device which generates an intense coherent beam of atoms through a stimulated process. It does for atoms what an optical laser does for light; whereas the optical laser emits coherent electromagnetic waves, the atom laser emits coherent matter waves. The condition of high intensity requires many particles per mode or quantum state. A thermal atomic beam has a population per mode of only 10^{-12} compared to values much greater than 1 for an atom laser. The realization of an atom laser therefore required methods to largely enhance the mode occupation. This was done by cooling to sub-microkelvin temperatures to the onset of Bose-Einstein condensation.

Laser light is created by stimulated emission of photons, a light amplification process. Similarly, an atom laser beam is created by stimulated amplification of matter waves. The conservation of the number of atoms is not in conflict with matter wave amplification: The atom laser takes atoms out of a reservoir and transforms them into a coherent matter wave similar to the manner in which an optical laser converts energy into coherent electromagnetic radiation. An atom laser is possible only for bosonic atoms because the accumulation of atoms in a single quantum state is a result of Bose-Einstein statistics. In a normal gas, atoms scatter among a myriad of possible quantum states. But when the critical temperature for Bose-Einstein condensation is reached, they scatter predominantly into the lowest energy state of the system. This abrupt process is closely analogous to the threshold for operation of an optical laser. The presence of a Bose-Einstein condensate causes stimulated scattering into the ground state. More precisely, the presence of a condensate with N_0 atoms enhances the probability that an atom will be scattered into the condensate by a factor of N_0+1 , in close analogy to the optical laser.

There is some ongoing discussion what *defines* a laser, even in the case of the optical laser[30, 31]; e.g. it has been suggested that stimulated emission is not necessary to obtain laser radiation[30]. In our discussion, we don't attempt to distinguish between defining features and desirable features of a laser.

Output coupler

A laser requires a cavity (resonator), an active medium, and an output coupler. Various "cavities" for atoms have been realized, but the most important ones are magnetic traps (which use the force of an inhomogeneous magnetic field on the atomic magnetic dipole moment) and optical dipole traps (which use the force exerted on atoms by focused laser beams).

The purpose of the output coupler is to extract atoms out of the cavity, thus generating a pulsed or continuous beam of coherent atoms. A simple way to accomplish this is to switch off the atom trap and release the atoms. This is analogous to cavity dumping for an optical laser and extracts all the stored atoms into a single pulse. A more controlled way to extract the atoms requires a coupling mechanism between confined quantum states and a propagating mode. Such a "beam splitter" for atoms was realized using the Stern-Gerlach effect (Fig. 10) [32]. A short rf pulse rotated the spin of the trapped atoms by a variable angle,

and the inhomogeneous magnetic trapping field separated the atoms into trapped and outcoupled components. By using a series of rf pulses, a sequence of coherent atom pulses could be formed (Fig. 11). The crescent shape of the propagating pulses can be qualitatively explained as the result of the forces of gravity and of the mean field. In the absence of gravity, one would expect a hollow shell or a loop propagating mainly in the radial direction; the center is depleted by the repulsion of the trapped condensate. However, the gravitational acceleration is 5.65 MHz/cm or 27 nK/ μm and is comparable to the maximum acceleration by the mean field. Therefore, atoms are not coupled out upward, resulting in a crescent instead of a loop. The two animations (Figs. 11 and 12), observed from the top and from the side, give a complete picture of the three-dimensional propagation of the outcoupled atom pulses.

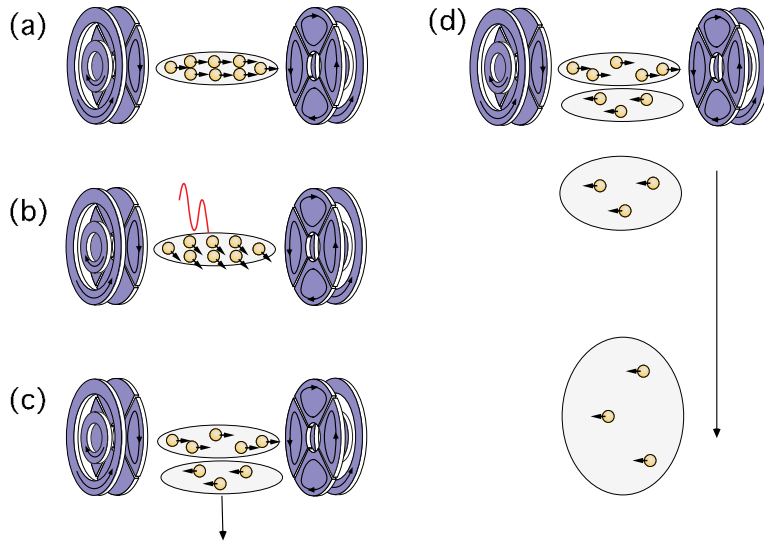


Fig. 10. The rf output coupler. Figure (a) shows a Bose condensate trapped in a magnetic trap. All the atoms have their (electron) spin up, i.e. parallel to the magnetic field. (b) A short pulse of rf radiation tilts the spins of the atoms. (c) Quantum-mechanically, a tilted spin is a superposition of spin up and down. Since the spin-down component experiences a repulsive magnetic force, the cloud is split into a trapped cloud and an out-coupled cloud. (d) Several output pulses can be extracted, which spread out and are accelerated by gravity.

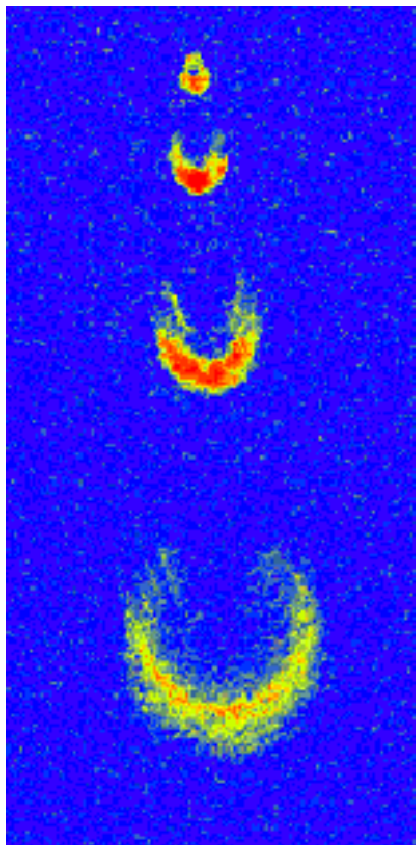


Fig. 11. The MIT atom laser operating at 200 Hz. The movie (field of view 1.8 mm x 3.9 mm) shows pulses of coherent sodium atoms coupled out from a Bose-Einstein condensate confined in a magnetic trap. Every five milliseconds, a short rf pulse rotated the magnetic moment of the trapped atoms, transferring a fraction of these atoms into a quantum state which is no longer confined ("non-magnetic" $m=0$ state). These atoms were accelerated downward by gravity and spread out. The atom pulses were observed by absorption imaging. Each of them contained between 10^5 and 10^6 atoms.

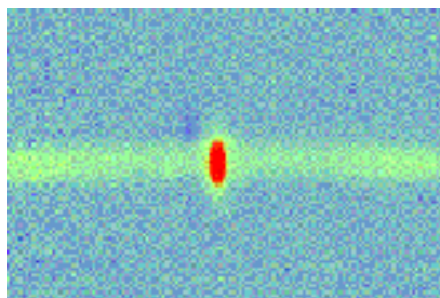


Fig. 12. Top view of the atom laser. This movie shows a single output pulse of the atom laser viewed from above with absorption imaging. The rf pulse used to outcouple atoms can put atoms into both of the untrapped magnetic states. This movie has finer time resolution than Fig. 11, allowing both the $m=1$ and $m=0$ outcoupled components to be observed. The $m=1$ component is strong field seeking, and is rapidly accelerated out of the magnetic trap. The $m=0$ component has very little interaction with the magnetic fields of the trap, so it expands almost ballistically and falls away from the camera under gravity, as seen in Fig. 11 (The lateral motion at the end of the top-view movie is due to the small angle between the probe light and the vertical axis).

Interference between two condensates

The spatial coherence of individual outcoupled pulses was proven in an interference experiment. Long range coherence is closely related to the existence of a macroscopic phase. As with any quantum mechanical phase, one cannot measure the absolute phase of a single atom laser pulse, but only the relative phase between two pulses. It is a non-trivial question whether two independent condensates have a well-defined relative phase. The analogous question for superfluids is this: If two superfluids are brought into a weak contact, is there a relative phase which would result in an observable dc Josephson current[33]? There is now general agreement that even if the phase is not initially defined, every realization of the experiment will show a distinct phase[34]. This is often called spontaneous symmetry breaking, and is a consequence of the quantum measurement process. In the case of two independent overlapping condensates one expects to observe a high-contrast interference pattern, but the phase of the pattern should randomly vary between different realizations.

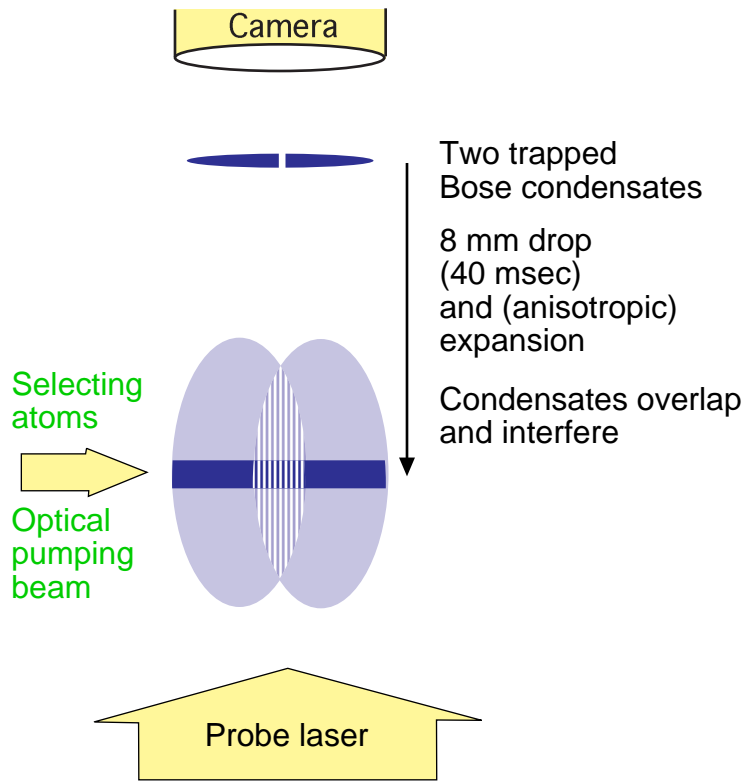


Fig. 13. Schematic setup for the observation of the interference of two Bose condensates, created in a double well potential. The two condensates were separated by a laser beam which exerted a repulsive force on the atoms. After switching off the trap, the condensates were accelerated by gravity, expanded ballistically, and overlapped. In the overlap region, a high-contrast interference pattern was observed by using absorption imaging. An additional laser beam selected absorbing atoms in a thin layer by optical pumping. This tomographic method prevented blurring of the interference pattern due to integration along the probe laser beam.

Two independent condensates were produced by evaporatively cooling atoms in a double-well potential. This potential was created by magnetic trap divided in half by optical forces of a focused far-off resonant laser beam. After the trap was switched off, the atom clouds fell down due to gravity, expanded ballistically, and eventually overlapped (Figs. 13 and 14). The interference pattern was observed using a resonant light beam which was absorbed

preferentially at the interference maxima[35]. As shown in Fig. 15, the interference pattern consisted of straight lines with a spacing of about $15\ \mu\text{m}$, a huge length for matter waves; the matter wavelength of atoms at room temperature is only $0.05\ \text{nm}$, less than the size of an atom. The interference experiment provided direct evidence for first-order coherence and long-range correlations, and for the existence of a relative phase of two condensates. Higher order coherences were observed in measurements of the internal energy of the condensate[36] and in measurements of three-body collisions[37]. All these studies were consistent with the standard assumption that a Bose condensate is coherent to first and higher order and can be characterized by a macroscopic wavefunction, but further studies are worthwhile and should lead to a more accurate characterization of the coherence properties of condensates.

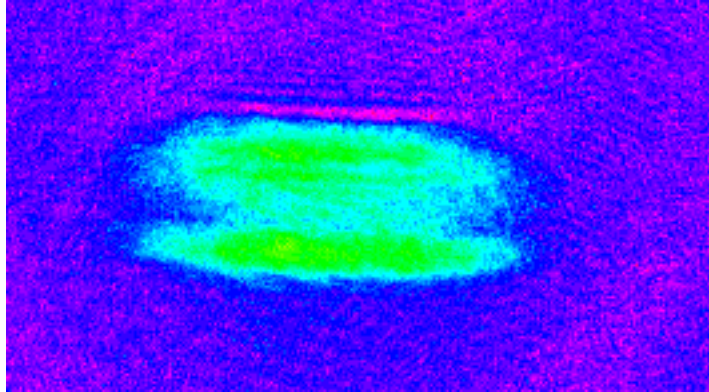


Fig. 14. Two expanding condensates. The first frames show a phase contrast picture of two trapped condensates, followed by their ballistic expansion after the magnetic trap has been turned off (observed with resonant absorption imaging). In the early frames, the absorption was saturated (red color) and the separation between the condensates is not visible. Since the trapped clouds were much more tightly confined in the radial direction, their internal energy was released mainly in the radial direction during expansion. The two condensates overlapped due to the slow axial expansion. After 40 msec, an interference pattern was observed (Fig. 15). The period of the interference fringes is the matter wavelength associated with the relative motion of the two condensates. Fringes are not visible in this movie because of the lower resolution and because of the blurring due to line-of-sight integration across the cloud (Fig. 13).

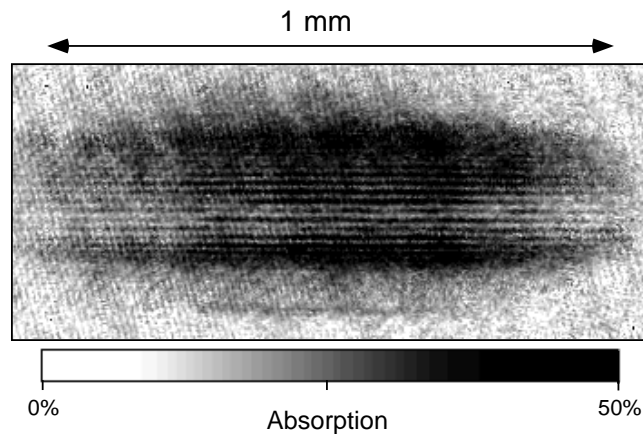


Fig. 15. Interference pattern of two expanding condensates observed after 40 msec time of flight. The width of the absorption image is $1.1\ \text{mm}$. The interference fringes have a spacing of $15\ \mu\text{m}$ and are strong evidence for the long-range coherence of Bose-Einstein condensates.

5. Conclusions

The basic phenomena of Bose-Einstein condensation in gases was predicted 70 years ago. The experimental realization required, first, the identification of an atomic system which would stay gaseous at the conditions of BEC and not preempt BEC by forming molecules or clusters, and second, the development of cooling and trapping techniques to reach those conditions. After this had been accomplished, several studies of BEC confirmed theories which had been formulated decades ago but had never been experimentally tested. But BEC has already gone beyond the confirmation of old theories; it has motivated several extensions of the theory. A microscopic picture has been developed of how a macroscopic phase is created [34]. Bose condensates might become a model system for dissipation and coherence in quantum systems. Different statistical ensembles have been discussed[38]. They agree in the thermodynamic limit but not for small Bose condensates. The theory of a weakly-interacting Bose gas has been extended to the situation of a harmonic trapping potential. The collapse of a condensate with attractive interactions has been studied, both theoretically[39, 40] and experimentally[3]. Furthermore, the direct visualization of macroscopic wavefunctions has added a very intuitive component to the understanding of many-body physics.

Finally, we want to mention some of the challenges ahead: to achieve quantum degeneracy for different atoms including fermionic isotopes, to study various mixtures of Bose condensates, to observe vortices, superfluidity, and Josephson tunneling, and to improve the output characteristics of the atom laser. Ultimately, Bose condensates and atom lasers should find use in atom optics and precision experiments.

Acknowledgments

We are grateful to our collaborators with whom the experiments have been carried out: M.R. Andrews, K.B. Davis, N.J. van Druten, S. Inouye, M.-O. Mewes, H.-J. Miesner, D.M. Stamper-Kurn, and C.G. Townsend. This work was supported by the Office of Naval Research, the National Science Foundation, Joint Services Electronics Program (ARO), and the David and Lucile Packard Foundation.